Streamer Head Observation in a Wire-Plate Electrode with Varied Wire Electrode Diameters

Y. Nagata[1], D. Wang[2], and T. Namihira[2]
[1]Graduate School of Science and Technology, Kumamoto University, Japan
[2]Institute of Pulse Power Science, Kumamoto University, Japan

Abstract—Effects of wire electrode diameter on formation and propagation process of streamer discharge in wire-plate electrode in air at atmospheric pressure were investigated using a high speed gated emICCD camera. Wire diameters of 0.2 mm, 1.0 mm and 2.0 mm were used in the study. Pulsed voltages having 100 ns pulse duration and about 90 kV peak voltage, generated by a Blumelein line generator, were applied to the electrodes with a gap fixed at 45 mm. Application of positive pulse voltages to the electrodes caused streamer discharges from wire to plate electrodes. During the streamer discharge, the formation and the propagation of streamer heads were observed. Increasing wire diameters from 0.2 mm to 2.0 mm resulted in the different streamer discharge parameters; propagation velocity of streamer heads from 1.48 mm/ns to 2.14 mm/ns, peak of discharge current from 139.9 A to 161.6 A, number density of streamer discharge reaching the plate electrode from 80 numbers/m to 55 numbers/m, respectively. Also, the streamer head diameter was changed. Therefore, it is concluded that the wire diameter is one of the important parameters to control the characteristics of the pulsed streamer discharge.

Keywords—Pulsed power, streamer discharge, streamer head, wire diameter, wire-plate electrode

I. Introduction

Streamer discharge plasma, a type of non-thermal plasma, has received global attention as a source of reactive radicals, and is used for many applications such as ozone generation, decomposition of NO_x and other gas pollutants, waste water treatment, disinfection, deodorization, and medical applications [1]–[4]. The tip of streamer discharge, which is called as the streamer head, in particular contributes to radical production. The peak electric field is located in the streamer head on the axis of symmetry of the discharge [5], likely resulting in many radical types. When performing treatment on gases using streamer discharge, the coaxial cylindrical electrode is generally used. Applying positive voltages to the electrodes, streamer head are formed on the central electrode and propagate directly to the outer electrode. Many streamer discharges are generated and they filled between the entire space of the electrode gap. Thus, the large volume of streamer discharges is able to treat large amounts of gases efficiently. Namihira et al. [1], [6], [7] have shown very remarkable results in NO removal efficiency and ozone generation yield using coaxial cylindrical electrodes. Improving gas treatment methods requires an understanding the characteristics of streamer discharge in the coaxial cylindrical electrode. Streamer discharge behaviors in axial direction of coaxial cylindrical electrodes have not been much reported.

The central (wire) electrode diameter in coaxial cylindrical electrode is considered a crucial parameter for streamer discharge formation and propagation because electric field strengths around the wire dramatically varies depending on a wire diameter. Formation and propagation of streamer discharge in wire-plate or -cylinder reactors have been studied in the literatures [8]–[22] but have rarely mentioned a wire diameter. Therefore, this study investigates effects of a wire electrode diameter on streamer discharges by observing the propagation process of streamer discharges in wire-plate electrodes.

Corresponding author: Takao Namihira
e-mail address: namihira@cs.kumamoto-u.ac.jp

II. Experimental apparatus and procedure

A. Pulsed power generator

Fig. 1 shows a schematic diagram of the pulsed power source used in the present work. The pulsed power source consisted of three Blumlein line generators and pulse transformer with a winding ratio of 1 to 3. Each Blumlein line generator was made by two coaxial cables (RG-213/U, Mitsubishi Cable Industries, Japan) which had a characteristic impedance of 50 Ω, respectively. Therefore, the characteristic impedance of the Blumlein line was calculated at 100 Ω. Here, three Blumlein line generator connected in parallel and then total characteristic impedance at the secondary side of the pulse transformer calculated by Eq. (1) resulted in $(100/3) \times 3^2 = 300\ \Omega$, where that Z_1, Z_2, N_1 and N_2 are characteristic

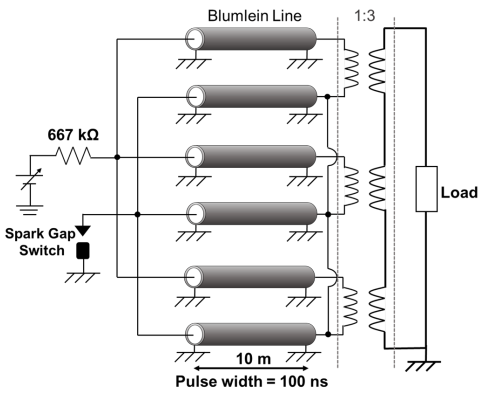

Fig. 1. Schematic diagram of pulsed power generator.

impedance and numbers of turns at the primary side and secondary side of the pulse transformer, respectively.

$$Z_2 = (N_2/N_1)^2 Z_1 \quad (1)$$

The length of the coaxial cable defines the pulse duration. In the work, 10 m long cables were employed and this corresponded to 100 ns of pulse duration. Charging voltage into the pulsed power source was fixed at 20 kV.

B. *Imaging system for pulsed discharge observation*

Fig. 2 shows a schematic diagram for imaging of the pulsed discharge. A pulsed power generator was used to generate the pulsed streamer discharges in the wire-plate electrode with 1.0 m length. To investigate the effects of wire diameter, three stainless wire electrodes having diameters of 0.2 mm, 1.0 mm and 2.0 mm, respectively, were used in this research. The plate electrode having a width of 10 mm was made of copper and was grounded. The gap from the center of wire electrode to the surface of plate electrode was fixed at 45 mm. Thus, the distance between the both surfaces of wire and plate electrodes had a difference of 0.9 mm at a maximum in the experiment. In the literature [21], Nakamura et al. showed that its difference was insignificant for streamer discharge process. The electrodes were installed in an acrylic case, and dry air at atmospheric pressure was fed into the case at a flow rate of 1.0 L/min. For all experiments, a positive voltage from the pulsed power generator was applied to the wire and was measured using a capacitive voltage divider. Current through the electrode was measured using a current transformer (Model CT-F2.5, Berogz instrumentation, USA), which was located just before the electrodes. A digital oscilloscope (RTO 1024, ROHDE & SCHWARZ, Germany) with a maximum bandwidth of 2 GHz and a maximum sample rate of 10 Gsamples/sec recorded the signals from the capacitive voltage divider and the current transformer. A high-speed gated emICCD camera (PI-MAX4:512EM, Princeton Instruments, USA) was used to observe the images of streamer discharges in the wire-plate electrode and was synchronized with the pulsed power generator. This camera can change the onset time of exposure itself. The exposure time of the camera was fixed at 5 ns and 100 ns in the experiments. To obtain streamer heads images clearly, discharge images were observed both 50 mm and 115 mm width of the wire-plate electrode, though a 1.0 m length electrode was employed as shown in Fig. 3. It should be mentioned that the capacitive voltage divider was handmade and was calibrated using a matched register to the pulsed power generator and the current transformer.

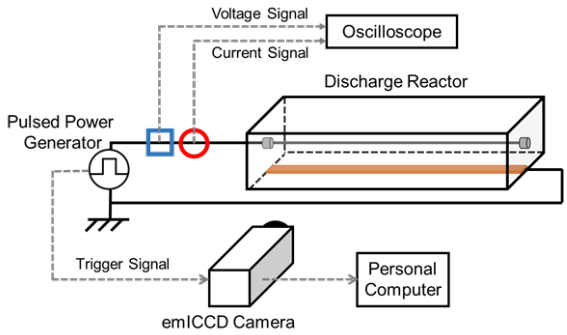

Fig. 2. Schematic diagram of the experimental apparatus.

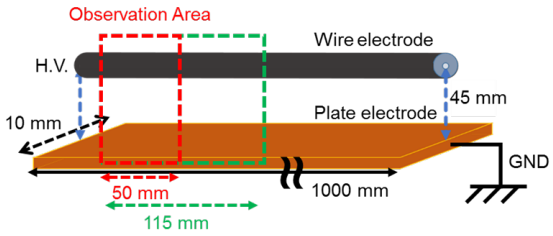

Fig. 3. Observation area in a wire-plate electrode.

III. Results and Discussion

A. *Waveform analysis*

The current waveform ($I_{\mathrm{measurement}}$ as shown in Eq. (2)), measured using a current transformer, includes both discharge current ($I_{\mathrm{discharge}}$) and displacement current ($I_{\mathrm{displacement}}$) into the electrode. Hence, calculating $I_{\mathrm{discharge}}$ requires to subtracting $I_{\mathrm{displacement}}$, calculated by Eq. (3), from $I_{\mathrm{measurement}}$, where $V_{\mathrm{measurement}}$ and $C_{\mathrm{electrode}}$ are the applied voltage to a wire and the capacitance of a wire-plate electrode obtained by Eq. (4), respectively. In Eq. (4), V and i show the voltage and the current with no discharge, respectively. The capacitances of the electrodes resulted in 8.1 pF, 10.7 pF and 12.3 pF with 0.2 mm, 1.0 mm and 2.0 mm wire, respectively.

$$I_{\mathrm{discharge}} = I_{\mathrm{measurement}} - I_{\mathrm{displacement}} \quad (2)$$

$$I_{\mathrm{displacement}} = C_{\mathrm{electrode}} \frac{\mathrm{d}V_{\mathrm{measurement}}}{\mathrm{d}t} \quad (3)$$

$$C_{\mathrm{electrode}} = \frac{1}{V} \int i \mathrm{d}t \quad (4)$$

Fig. 4 shows typical waveforms of applied voltages, $V_{\mathrm{measurement}}$ (a) to and discharge currents, $I_{\mathrm{discharge}}$ (b) into the electrodes having different wire diameters. The output voltage from the pulsed power generator was applied at $t = 0$. Table I shows a summary of peak voltages, peak currents and voltage rise rates under each electrode. Here, voltage rise time was defined as the time required to raising from 10% to 90% of the peak voltage. Percentages reflect the ratios on the basis of 0.2 mm wire electrode. A wire electrode with thicker diameter led an increment of peak current while peak voltage was kept at 90 kV. In Fig. 4, before and after the peak of applied voltage, the discharge currents were divided into two phases. The applied voltage reached to the peak (55.0 ns), then the discharge current increased sharply. In two phases, the primary and secondary phases were discriminated between streamer and glow discharges (sometimes called as primary and secondary streamers) in the literature [23]. Fig. 5 shows discharge currents under each electrode focused on the streamer discharge phase. During streamer discharge phase, an electrode with thicker wire led the increment of discharge current and the delay of discharge current onset.

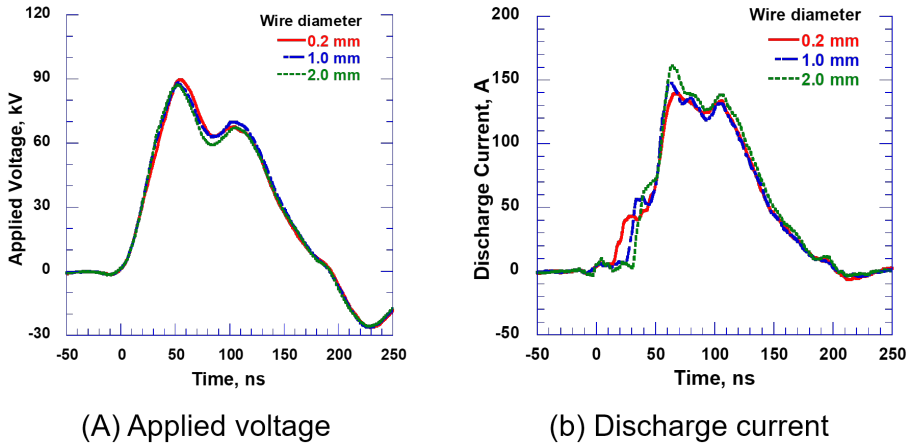

Fig. 4. Typical waveforms of voltages and currents.

TABLE I
SUMMARY OF PEAK VOLTAGE AND PEAK CURRENT AND VOLTAGE RISE RATE

Wire diameter [mm]	0.2	1.0	2.0
Peak voltage [kV]	89.9 (100%)	88.4 (98.3%)	87.4 (97.2%)
Peak current [A]	139.9 (100%)	148.6 (106.2%)	161.6 (115.5%)
Voltage rise rate [kV/ns]	1.92 (100%)	1.94 (101.0%)	2.03 (105.7%)

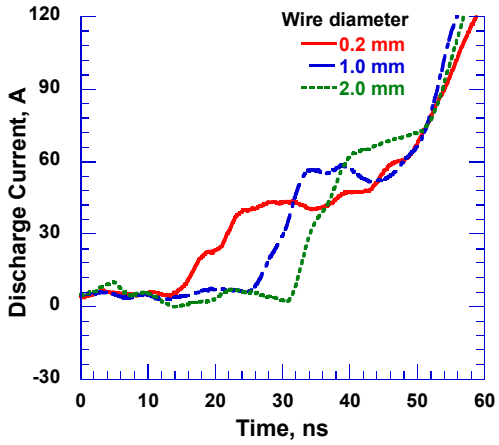

Fig. 5. Discharge currents focused on the streamer discharge phase.

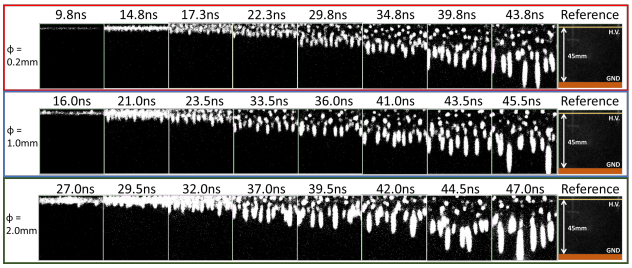

Fig. 6. Images of streamer heads propagation for different wire diameter.

B. *Imaging of streamer discharge*

Fig. 6 shows images of emissions from streamer discharges as a function of time in different wire diameters of 0.2 mm, 1.0 mm and 2.0 mm. The images were observed using an emICCD camera with 5 ns of exposure time. Times of each image indicate the onset time of exposure from the application of pulse voltage ($t = 0$). Bright areas of the images show the trace of streamer discharge during exposure time. Brightness degree reflects the emission intensity. In the experiments, all images were photographed using the identical gain of emICCD camera. As shown in Fig. 6, the streamer heads propagate from the wire to the plate. The first frames, recognizing discharge emission in vicinity of each wire, were taken at 9.8–14.8 ns, 16.0–21.0 ns and 27.0–32.0 ns, respectively. The fully developed streamer discharge between the electrode were observed in the frames snapped at 43.8–48.8 ns, 40.5–45.5 ns and 47.0–52.0 ns under each electrode condition, respectively. These times approximately matched to the transition time of the discharge currents in Fig. 5. From the results, the current increases along with streamer heads propagation, and then it increases sharply after streamer heads reached the plate electrode. This is because that the streamer heads propagate with a higher density of ionization [6] and then the streamer discharges connect between wire and plate electrodes with higher conductivity plasma channel.

C. *Streamer head velocity and diameter*

Streamer head positions relative to the wire as a function of time were determined by images shown in Fig. 6. The time dependences of streamer head position for different wire diameters are shown in Fig. 7. As shown in Fig. 7, the propagation velocities of streamer head for all wire diameters grow faster as with proceeding to plate electrode. The acceleration of streamer head propagation might be caused by

TABLE II
STREAMER HEADS AVERAGE VELOCITY

Wire diameter [mm]	0.2	1.0	2.0
Average velocity of streamer head [mm/ns]	1.48 (100%)	1.85 (124.8%)	2.14 (144.4%)

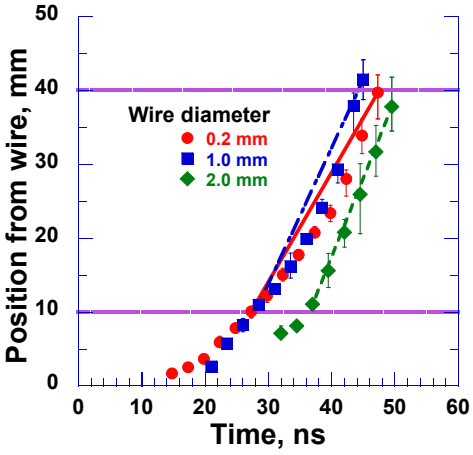

Fig. 7. Streamer head positions from the wire as a function of time.

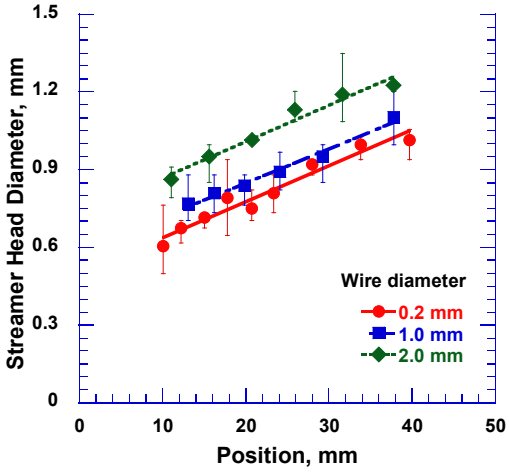

(a) Position

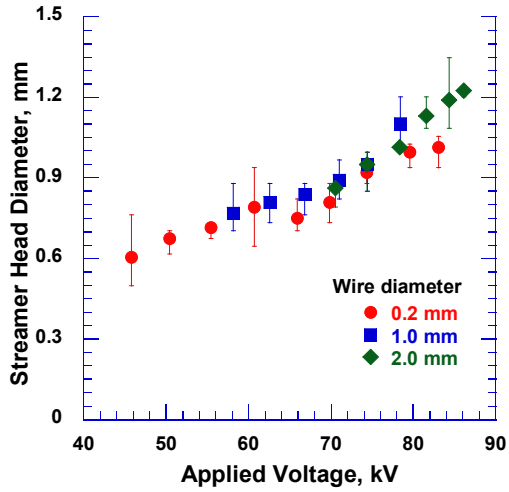

(b) Applied voltage

Fig. 8. Streamer head diameters as a function of position from wire electrode and applied voltage to wire electrode.

the enhancement of the electric field between a streamer head and the plate electrode with shortening their distance.

The average velocity of streamer head was approximated from the inclinations between 10 mm and 40 mm of positions from the wire and was summarized in Table II. It is noted that the influences of the electric field of wire electrode and the final jump phenomenon [24] of streamer head were removed from the average velocity of streamer head. Table II includes the average velocities of streamer head for different wire diameters. Percentage values under each velocity reflect the ratios to 0.2 mm wire diameter. From Fig. 7 and Table II, the average velocity of streamer head become faster with thicker wire electrode. It is considered that the applied voltage to wire electrode during streamer propagation was larger in case of thicker wire since the onset of streamer discharge was delayed. Streamer head velocity might be determined by its electric field strength as the attraction force of electron avalanches. Therefore, the higher applied voltage to wire electrode make the streamer head to have the higher electric field strength. Accordingly, in this work, it is clear that the average velocity of streamer head is affected by the applied voltage to wire electrode during its propagation and become faster with thicker wire due to the delay of streamer discharge inception.

From Fig. 6, the diameter of streamer head was also determined. The streamer head diameter as a functions of the position from and the applied voltage to wire electrode was shown in Fig. 8 (a) and (b). In Fig. 8 (a), the diameter of streamer head grows during its propagation to plate electrode in all cases of wire electrode diameter. In addition, the thicker wire electrode provides the bigger diameter of streamer head. Generally, it is known by the simulation works [25], [26] that the electric field strength of streamer head is reflected in its propagation velocity and its size. The results in Table II and Fig. 8 (a) follows the knowledge suggested by the computer simulations. From Fig. 8 (b), it is seemed that the diameter of streamer head during its propagation is strongly influenced by the voltage applied to wire electrode. This is because that the streamer head has connection to the wire electrode with the conductivity plasma channel.

D. Streamer head formation and propagation

Fig. 9 (a)–(c) shows streamer propagation images corresponding to current waveform for different wire diameters of 0.2 mm, 1.0 mm and 2.0 mm, respectively. Times above each image indicate the onset time of camera exposure. Dotted lines indicate the exposure onset time corresponding to each

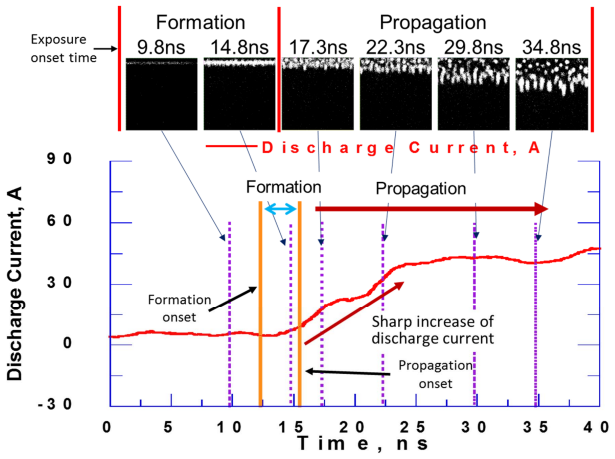

(a) 0.2 mm of wire diameter

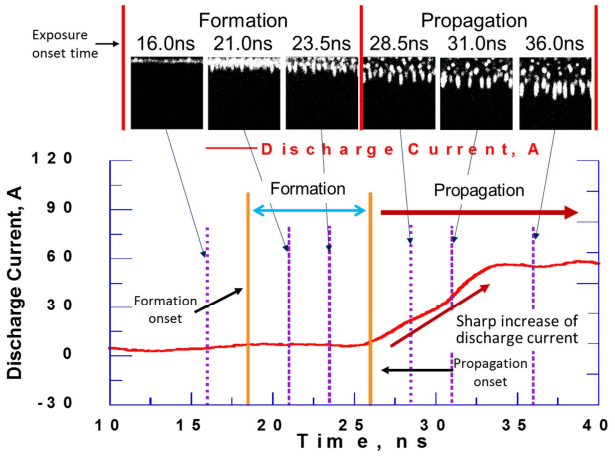

(b) 1.0 mm of wire diameter

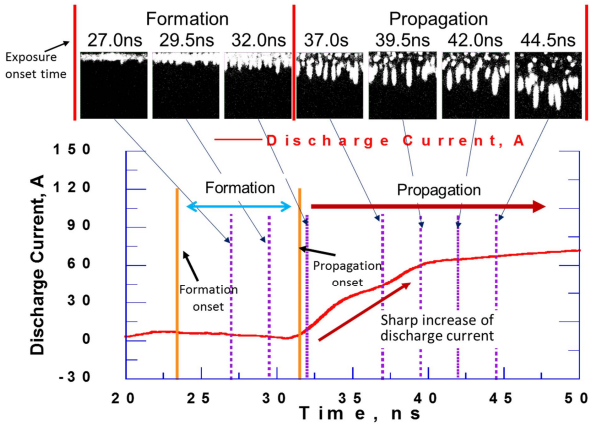

(c) 2.0 mm of wire diameter

Fig. 9. Streamer propagation images corresponding to the current waveform.

image. As shown in Fig. 9 (a), on the images photographed from 9.8 ns and 14.8 ns, the emission from streamer head was observed in the vicinity of wire electrode. In contrast, on the image taken from 17.3 ns, the emission in the vicinity of wire ceased and streamer heads got away from wire electrode

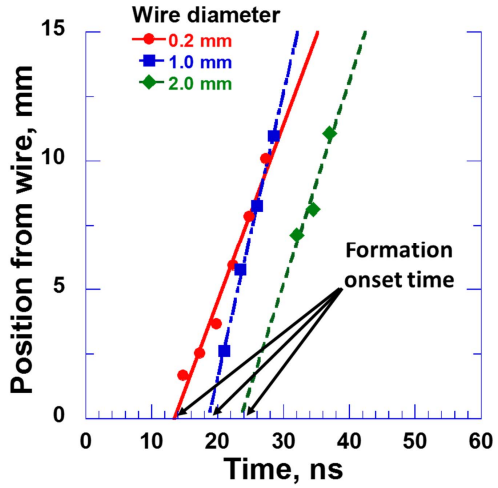

Fig. 10. Streamer head positions from the wire as a function of time modified from Fig. 7.

TABLE III
ONSET TIMES OF STREAMER HEADS FORMATION AND PROPAGATION

Wire diameter [mm]	0.2	1.0	2.0
Formation onset time [ns]	12.3	18.5	23.4
Propagation onset time [ns]	15.5	26.5	31.5

with a sharp increase of the discharge current. The same trend is observed in Fig. 9 (b) and (c). Therefore, in this report, the time period observing the emission in the vicinity of the wire electrode is defined as the streamer head formation and the time of an initial increasing of the discharge current is defined as the onset of the streamer head propagation.

For find out the onset time of streamer head formation, Fig. 7 was analyzed in detail. Fig. 10 indicates the enlarged figure of Fig. 7 along with vertical axis "Position from wire". All symbols in Fig. 10 were derived from the emICCD images taken before the propagation of streamer head. In Fig. 10, the intercept value determined on the axis of "Time" is considered as the onset time of streamer head formation. The onset times for the formation and the propagation of streamer head estimated from Fig. 10 and Fig. 9, respectively, were summarized in Table III. From Table III, the thicker wire makes longer lags from the voltage application for the formation and the propagation of streamer head and lead longer period of streamer head formation.

A summary of the applied voltage to and the electric field strength on the wire electrode at the onset times of the streamer head formation and the propagation were shown in Table IV. The electric field strength was calculated using Eq. (5) [27], where that V, h and r are applied voltage, distance between electrodes, and wire radius, respectively.

$$E_0 = \frac{2\sqrt{h^2 - R^2}}{\left\{h^2 - R^2 - (h-R)^2\right\} \ln \frac{h+\sqrt{h^2-R^2}}{R}} \quad (5)$$

Table IV show that, in case of the thinner wire electrode, the electric field strength on the wire, when the streamer head was formed around and leaved from the wire, become higher

TABLE IV
APPLIED VOLTAGE AND ELECTRIC FIELD AT THE ONSET TIMES OF STREAMER HEADS FORMATION AND PROPAGATION

(a) Formation onset

Wire diameter [mm]	0.2	1.0	2.0
Time [ns]	12.3	18.5	23.4
Applied voltage [ns]	15.8	29.1	39.9
Electric field [kV/mm]	23.3	11.3	9.1

(b) Propagation onset

Wire diameter [mm]	0.2	1.0	2.0
Time [ns]	15.5	26.0	31.5
Applied voltage [ns]	22.3	45.9	60.6
Electric field [kV/mm]	32.9	17.9	13.8

though the applied voltage to the wire was small. From the facts, it is indicated that the formation and the propagation onsets are more highly affected by the electric field strength on the wire than by the applied voltage. Here, it is noted that the whisker effect become stronger with the thicker diameter of wire electrode. Hence, it is possibility that the electric field strength on thicker wire is really much higher than the calculated value shown in Table IV.

E. Streamer head density

Streamer head density as a function of time was determined by the images shown in Fig. 6 and was shown in Fig. 11. From Fig. 11, the density of streamer head decreases during its propagation from the wire to the plate electrodes for all case of wire diameter. On the other hand, the size of streamer head grow wider during its propagation as shown in Fig. 8. Additionally, the images of the streamer discharge photographed using emICCD camera with long exporsure time (100 ns) and wide width (115 mm) are shown in Fig. 12. It is clearly understood from Fig. 12 that some streamer heads gradually merged and they become the bigger one during the propagation. The phenomenon is one of the reason why the density of streamer head decrease and the size of streamer head increases during the propagation. For the applications of the pulsed streamer discharge to the gaseous treatment, the uniformity of discharge plasma is one of the important properties. Here, using the images in Fig. 12, the area ratio of emission from streamer discharge to gap apace in wire-plate electrode was indicated in Fig. 13. The ratio of emission to gap space slightly reduces with the expanding the diameter of wire electrode. Typically, the ratio derived from 2.0 mm wire is approximately 3% smaller compared with one derived from 0.2 mm wire even though the density of streamer head reached to the plate electrode is 33% smaller. This is because that the size of streamer head in the case of 2.0 mm wire is 20% bigger than that of 0.2 mm wire.

IV. INTERPRETATION

In the work, the detail influence of wire diameter in wire-plate discharge electrode with the application of pulsed power was investigated. The thinner wire has the higher electric field compared with the thicker one at the same applied voltage and

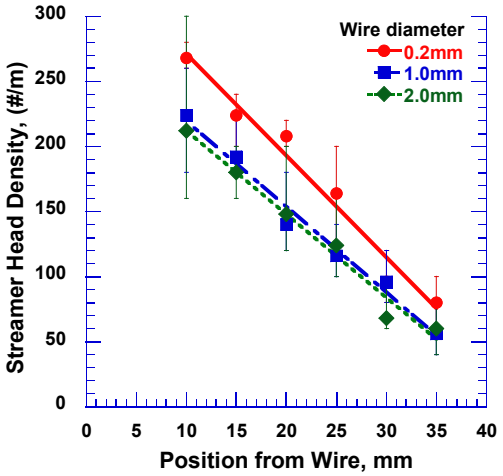

Fig. 11. Density of streamer head as a function of position from wire electrode.

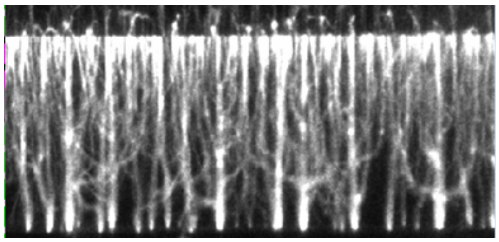

(a) 0.2 mm of wire diameter

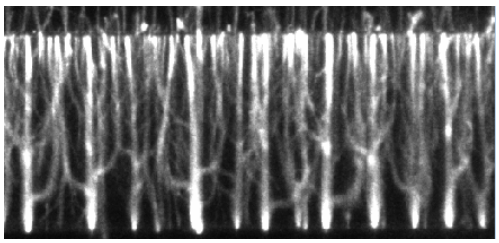

(b) 1.0 mm of wire diameter

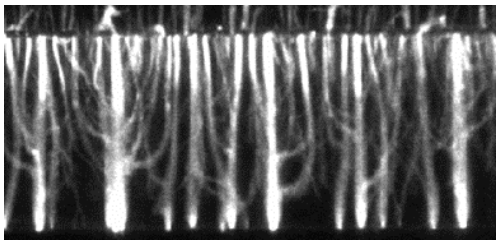

(c) 2.0 mm of wire diameter

Fig. 12. Propagation images of streamer head photographed using emICCD camera with 100 ns exposure time and 115 mm width.

therefore the streamer head in the vicinity of thinner wire is generated earlier. However, the streamer head formed around the thinner wire has the smaller velocity and diameter during its propagation since the applied voltage to wire electrode is lower. On the other hand, the streamer head produced around the thicker wire propagates with the higher velocity and has larger size. From the results, in the wire-plate electrode, the

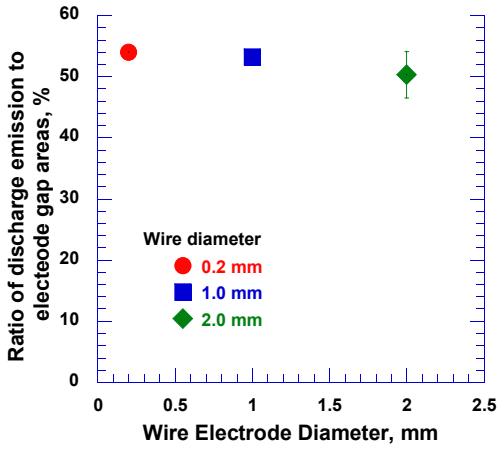

Fig. 13. Ratio of emission area to electrode gap area.

wire diameter has the strong effects on the formation and the propagation of the streamer head. In other words, the electric field strength on the wire electrode effects on the formation of streamer head and the applied voltage on the wire electrode influences the propagation of streamer head.

In addition, during the formation of the streamer heads in the vicinity of wire electrode, the plenty of heads are generated in the case of using thinner wire. During the propagation of the streamer heads from the wire to plate electrodes, some of the streamer heads merge together and grow to large size in both cases of using thinner and thicker wires. From the view point of the discharge homogeneity in the reactor, the thinner wire electrode has the better performance than the thicker wire.

V. Summary

Effects of the wire electrode diameter on streamer head formation and propagation in a wire-plate electrode were investigated using an emICCD camera. Results are summarized as follows. Thicker wire led to:

1) Delay of streamer head formation and propagation from pulsed power application;
2) Increasing of discharge current during streamer head propagation;
3) Faster average propagation velocity of streamer head;
4) Bigger diameter and lower density of streamer head;
5) Lower uniformity of discharge plasma.

Though streamer heads generated by thicker wire have the higher electric fields, they have smaller treatment volume of gases. On the other hand, though streamer heads generated by thinner wire have larger treatment volume, their electric field is smaller. Therefore, the selection of wire diameter in wire-plate or wire-cylinder electrode (= enhancement factor of reactor) is required for better performance of applications.

References

[1] T. Namihira, S. Tsukamoto, D. Wang, S. Katsuki, R. Hackam, H. Akiyama, Y. Uchida, and M. Koike, "Improvement of NO_x removal efficiency using short-width pulsed power," *IEEE Transactions on Plasma Science*, vol. 28, pp. 434–442, 2000.

[2] A. Ogasawara, J. Han, K. Fukunaga, J. Wang, D. Wang, T. Namihira, M. Sasaki, H. Akiyama, and P. Zhang, "Decomposition of toluene using nanosecond-pulsed-discharge plasma assisted with catalysts," *IEEE Transactions on Plasma Science*, vol. 43, pp. 3461–3469, 2015.

[3] D. Wang, T. Matsumoto, T. Namihira, and H. Akiyama, "Development of higher yield ozonizer based on nano-seconds pulsed discharge," *Journal of Advanced Oxidation Technologies*, vol. 13, pp. 71–78, 2010.

[4] A. Komuro, R. Ono, and T. Oda, "Behaviour of OH radicals in an atmospheric-pressure streamer discharge studied by two-dimensional numerical simulation," *Journal of Physics D: Applied Physics*, vol. 46, p. 175206, 2013.

[5] Z. Bonaventura, A. Bourdon, S. Celestin, and V. Pasko, "Electric field determination in streamer discharges in air at atmospheric pressure," *Plasma Sources Science and Technology*, vol. 20, p. 035012, 2011.

[6] D. Wang, T. Namihira, and H. Akiyama, "Recent progress of nano-seconds pulsed discharge and its applications," *Journal of Advanced Oxidation Technologies*, vol. 14, pp. 131–137, 2011.

[7] T. Matsumoto, D. Wang, T. Namihira, and H. Akiyama, "Energy efficiency improvement of nitric oxide treatment using nanosecond pulsed discharge," *IEEE Transactions on Plasma Science*, vol. 38, pp. 2639–2643, 2010.

[8] G. J. J. Winands, Z. Liu, A. J. M. Pemen, E. J. M. Van Heesch, and K. Yan, "Analysis of streamer properties in air as function of pulse and reactor parameters by ICCD photography," *Journal of Physics D: Applied Physics*, vol. 41, p. 234001, 2008.

[9] T. Kuroki, M. Takahashi, M. Okubo, and T. Yamamoto, "Single-stage plasma-chemical process for particulates, NO_x, and SO_x simultaneous removal," *IEEE Transactions on Industry Applications*, vol. 38, pp. 1204–1209, 2002.

[10] M. Okubo, G. Tanioka, T. Kuroki, and T. Yamamoto, "NO_x concentration using adsorption and nonthermal plasma desorption," *IEEE Transactions on Industry Applications*, vol. 38, pp. 1196–1203, 2002.

[11] B. S. Rajanikanth and V. Ravi, "Pulsed electrical discharges assisted by dielectric pellets/catalysts for diesel engine exhaust treatment," *IEEE Transactions on Dielectrics and Electrical Insulation*, vol. 9, pp. 616–626, 2002.

[12] H. H. Kim, K. Tsunoda, S. Katsura, and A. Mizuno, "A novel plasma reactor for NO_x control using photocatalyst and hydrogen peroxide injection," *IEEE Transactions on Industry Applications*, vol. 35, pp. 1306–1310, 1999.

[13] J.-D. Moon, G.-T. Lee, and S.-H. Chung, "SO_2 and CO gas removal and discharge characteristics of a nonthermal plasma reactor in a crossed DC magnetic field," *IEEE Transactions on Industry Applications*, vol. 35, pp. 1198–1204, 1999.

[14] Y. S. Mok and I.-S. Nam, "Positive pulsed corona discharge process for simultaneous removal of SO_2 and NO_x from iron-ore sintering flue gas," *IEEE Transactions on Plasma Science*, vol. 27, pp. 1188–1196, 1999.

[15] T. Oda, T. Kato, T. Takahashi, and K. Shimizu, "Nitric oxide decomposition in air by using nonthermal plasma processing with additives and catalyst," *IEEE Transactions on Industry Applications*, vol. 34, pp. 268–272, 1998.

[16] B. E. J. M. V. Heesch, G. U. A. J. M. Pemen, K. Yan, S. V. B. V. Paasen, K. J. Ptasinski, and P. A. H. J. Huijbrechts, "Pulsed corona tar cracker," *IEEE Transactions on Plasma Science*, vol. 28, pp. 1571–1575, 2000.

[17] G. Prieto, O. Prieto, C. R. Gay, and T. Yamamoto, "Destruction of residual fumigant using a plasma reactor," *IEEE Transactions on Industry Applications*, vol. 39, pp. 72–78, 2003.

[18] Y. Yankelevich and A. Pokryvailo, "High-power short-pulsed corona: investigation of electrical performance, SO_2 removal, and ozone generation," *IEEE Transactions on Plasma Science*, vol. 30, pp. 1975–1981, 2002.

[19] S. Iwasaki, Y. Murata, D. Ito, Y. Ehara, H. Kishida, and T. Ito, "Improvement of NO_x removal rate using discharge, photocatalyst and UV rays (in Japanese)," *IEEJ Transactions on Fundamentals and Materials*, vol. 124, pp. 909–914, 2004.

[20] T. Huiskamp, W. Sengers, F. J. C. M. Beckers, S. Nijdam, U. Ebert, E. J. M. van Heesch, and A. J. M. Pemen, "Spatiotemporally resolved imaging of streamer discharges in air generated in a wire-cylinder reactor with (sub)nanosecond voltage pulses," *Plasma Sources Science and Technology*, vol. 26, p. 075009, 2017.

[21] K. Nakamura, D. Wang, and T. Namihira, "Behavior of pulsed streamer discharge in a wire-plate electrode with varied gap distances," *International Journal of Plasma Environmental Science and Technology*, vol. 11, pp. 98–103, 2017.

[22] A. Mizuno, K. Shimizu, S. Furuta, A. Chakrabarti, and L. Dascalescu, "NO_x removal process using pulsed discharge plasma," *IEEE Transactions on Industry Applications*, vol. 31, pp. 957–962, 1995.

[23] T. Namihira, D. Wang, S. Katsuki, R. Hackam, and H. Akiyama, "Propagation velocity of pulsed streamer discharges in atmospheric air," *IEEE Transactions on Plasma Science*, vol. 31, pp. 1091–1094, 2003.

[24] H. Pépin, D. Comtois, F. Vidal, C. Y. Chien, A. Desparois, T. W. Johnston, J. C. Kieffer, B. L. Fontaine, F. Martin, F. A. M. Rizk, C. Potvin, P. Couture, H. P. Mercure, A. Bondiou-Clergerie, P. Lalande, and I. Gallimberti, "Triggering and guiding high-voltage large-scale leader discharges with sub-joule ultrashort laser pulses," *Physics of Plasmas*, vol. 8, pp. 2532–2539, 2001.

[25] F. Tochikubo and H. Arai, "Numerical simulation of streamer propagation and radical reactions in positive corona discharge in N_2/NO and N_2/O_2/NO," *Japanese Journal of Applied Physics*, vol. 41, pp. 844–852, 2002.

[26] A. Komuro, K. Takahashi, and A. Ando, "Numerical simulation for the production of chemically active species in primary and secondary streamers in atmospheric-pressure dry air," *Journal of Physics D: Applied Physics*, vol. 48, p. 215203, 2015.

[27] H. Hara and H. Akiyama, *High-Voltage Pulsed Power Engineering (in Japanese)*. Tokyo, Japan: Morikita Publishing, 2011, pp. 9–10.